

## Ultra-Slow Inactivation in $\mu 1$ Na<sup>+</sup> Channels Is Produced by a Structural Rearrangement of the Outer Vestibule

Hannes Todt,\* Samuel C. Dudley, Jr.,# John W. Kyle,§ Robert J. French,<sup>¶</sup> and Harry A. Fozzard<sup>§</sup>

\*Institute of Pharmacology of the University of Vienna, 1090 Vienna, Austria; #Division of Cardiology, Emory University/VAMC, Decatur, Georgia 30033 USA; §Cardiac Electrophysiology Laboratories and the Departments of Pharmacological and Physiological Sciences and Medicine, The University of Chicago, Chicago, Illinois 60637 USA; and <sup>¶</sup>Department of Physiology and Biophysics, University of Calgary, Calgary, Alberta T2N 4N1, Canada

**ABSTRACT** While studying the adult rat skeletal muscle Na<sup>+</sup> channel outer vestibule, we found that certain mutations of the lysine residue in the domain III P region at amino acid position 1237 of the  $\alpha$  subunit, which is essential for the Na<sup>+</sup> selectivity of the channel, produced substantial changes in the inactivation process. When skeletal muscle  $\alpha$  subunits ( $\mu 1$ ) with K1237 mutated to either serine (K1237S) or glutamic acid (K1237E) were expressed in *Xenopus* oocytes and depolarized for several minutes, the channels entered a state of inactivation from which recovery was very slow, i.e., the time constants of entry into and exit from this state were in the order of  $\sim 100$  s. We refer to this process as “ultra-slow inactivation.” By contrast, wild-type channels and channels with the charge-preserving mutation K1237R largely recovered within  $\sim 60$  s, with only 20–30% of the current showing ultra-slow recovery. Coexpression of the rat brain  $\beta 1$  subunit along with the K1237E  $\alpha$  subunit tended to accelerate the faster components of recovery from inactivation, as has been reported previously of native channels, but had no effect on the mutation-induced ultra-slow inactivation. This implied that ultra-slow inactivation was a distinct process different from normal inactivation. Binding to the pore of a partially blocking peptide reduced the number of channels entering the ultra-slow inactivation state, possibly by interference with a structural rearrangement of the outer vestibule. Thus, ultra-slow inactivation, favored by charge-altering mutations at site 1237 in  $\mu 1$  Na<sup>+</sup> channels, may be analogous to C-type inactivation in *Shaker* K<sup>+</sup> channels.

### INTRODUCTION

The outer vestibule of voltage-gated Na<sup>+</sup> channels is formed by four extracellular loops that connect transmembrane segments 5 and 6 in each of the domains. These segments fold back into the membrane to form part of the ion permeation pathway (Guy and Conti, 1990; Lipkind and Fozzard, 1994; Chiamvimonvat et al., 1996a, b; Pérez-García et al., 1996). At the turn of the domain III loop within the membrane, the highly conserved amino acid K1237 (amino acid numbering corresponds to  $\mu 1$ , the adult rat skeletal muscle isoform) has been identified as part of the selectivity filter of the channel (Lipkind and Fozzard, 1994; Favre et al., 1996) based on studies showing that mutations of this residue profoundly alter the channel's ion selectivity (Heinemann et al., 1992; Chiamvimonvat et al., 1996a; Favre et al., 1996; Pérez-García et al., 1996; Tsushima et al., 1997). Amino acids located in the outer vestibule may contribute to channel gating, in addition to the control of ion permeation. Tomaselli and his colleagues reported that the mutation W402C eliminated slow inactivation in  $\mu 1$  Na<sup>+</sup> channels (Tomaselli et al., 1995; Balser et al., 1996). *Shaker* K<sup>+</sup> channels, as well as Na<sup>+</sup> channels, exhibit several different inactivation processes. Mutations

in the outer pore region of the *Shaker* K<sup>+</sup> channel have been shown to alter a slower process called “C-type” inactivation (Hoshi et al., 1991; López-Barneo et al., 1993). This C-type inactivation can also be altered by charged pore-blocking agents such as cadmium (Yellen et al., 1994) or tetraethylammonium (Grissmer and Cahalan, 1989; Choi et al., 1991).

While performing mutational studies of K1237 we found that alteration of charge at that location induced a prominent inactivated state from which recovery was very slow. This inactivation process showed similar features to C-type inactivation in *Shaker* K<sup>+</sup> channels because it was suppressed by the presence of an extracellular pore-blocking ligand, the mutant  $\mu$ -conotoxin GIIIA ( $\mu$ -CTX), R13Q.  $\mu$ -CTX R13Q was used because it only partially blocks single channel current (Becker et al., 1992), thus allowing channel gating mechanisms to be studied when all channels are occupied by toxin (French et al., 1996). Preliminary reports of this work have been published in abstract form (Todt et al., 1997a, b).

### METHODS

The adult rat skeletal muscle clone,  $\mu 1$ -2, was the gift of Gail Mandel (SUNY; Trimmer et al., 1989). We also used a *Xenopus* globin expression vector,  $\mu 1$ -pAlter XG, consisting of the  $\mu 1$  coding sequence flanked by *Xenopus* globin 5' and 3' untranslated regions in pAlter (Promega, Madison, WI). The  $\mu 1$ -pAlter XG construct was provided as a gift by Randall Moorman and Edward Johns (University of Virginia). The mutations of the lysine residue at amino acid position 1237 to Arg (K1237R), Ser (K1237S), and Glu (K1237E) were made by three primer PCR (Bowman et al., 1990). Oligonucleotides (length: 40mers) were designed to contain the desired

Received for publication 26 February 1998 and in final form 12 November 1998.

Address reprint requests to Dr. Hannes Todt, Institute of Pharmacology, University of Vienna, Waehringerstrasse 13a, 1090 Vienna, Austria. Tel.: +43-1-4277-64137; Fax: +43-1-4277-9641; E-mail: hannes.todt@univie.ac.at.

© 1999 by the Biophysical Society

0006-3495/99/03/1335/11 \$2.00

amino acid mutation and an additional mutation which introduced a silent *PstI* restriction site without altering amino acid coding sequence. The outside PCR primers used in the three primer PCR mutagenesis reactions produced a fragment that encompassed unique *AatII* (3292 nt) and *SacII* (4365 nt) restriction sites. PCR products were digested with *AatII* and *SacII*, and the resulting 1070-bp fragment was gel-purified and directionally subcloned into the same unique *AatII* and *SacII* restriction sites of a modified  $\mu 1$ -2 construct. The entire PCR-generated *AatII* to *SacII* region was sequenced to verify the presence of the desired mutations as well as the absence of spurious mutations. The region containing the desired mutation was subsequently shuttled to  $\mu 1$ -pAlter XG, which consistently gave higher levels of expression, using unique *BssHII* (2075 nt) to *SacII* (4365 nt) sites. The  $\mu 1$  constructs were linearized for preparation of RNA transcript by *SalI* digestion and transcribed with SP6 DNA-dependent RNA polymerase (New England Biolabs, Beverly, MA) using reagents from the mCAP RNA Capping Kit (Stratagene, La Jolla, CA). The rat brain  $\beta 1$  subunit of the  $\text{Na}^+$  channel was also subcloned into pAlterXG and transcription prepared from *BamHI* linearized template using SP6 RNA polymerase (Makielski et al., 1996).

Stage V and VI *Xenopus* oocytes were isolated from female frogs (NASCO, Ft. Atkinson, WI), washed with  $\text{Ca}^{2+}$ -free solution (90 mM NaCl, 2.5 mM KCl, 1 mM  $\text{MgCl}_2$ , 1 mM  $\text{NaH}_2\text{PO}_4$ , and 5 mM HEPES titrated to pH 7.6 with 1 N NaOH), treated with 2 mg/ml collagenase (Sigma, St. Louis, MO) for 1.5 h, and had their follicular cell layers manually removed. Approximately 50–100 ng of cRNA was injected into each oocyte with a Drummond microinjector (Broomall, PA). Oocytes were incubated at 16°C for 12 h to 3 days before examination.

Recordings were made in the two-electrode voltage clamp configuration using a Dagan CA-1 voltage clamp (Dagan, Minneapolis, MN). All recordings were obtained at room temperature (20–22°C). Recordings were made in a bathing solution that consisted of (in mM): 90 NaCl, 2.5 KCl, 1  $\text{BaCl}_2$ , 1  $\text{MgCl}_2$ , and 5 mM HEPES titrated to pH 7.2 with 1 N NaOH.  $\text{BaCl}_2$  was used to minimize  $\text{Ca}^{2+}$ -activated  $\text{Cl}^-$ -currents that arose as a consequence of  $\text{Ca}^{2+}$  entry via some of the mutant channels. Oocytes were placed in recording chambers in which the bath flow rate was 100 ml/h, and the bath level was adjusted so that the total bath volume was <500  $\mu\text{l}$ . Electrodes were filled with 3 M KCl and had resistances of <1 M $\Omega$ . The peak inward currents studied were in the range between ~1 and 7  $\mu\text{A}$ . Using pCLAMP6 (Axon Instruments, Foster City, CA) software, data were acquired at 71.4 kHz after low-pass filtration at 2 kHz (–3dB). Curve fitting was performed using ORIGIN 3.5 (MicroCal Software, Inc., Northampton, MA). The nonlinear least-squares regression method was based on the Levenberg-Marquardt algorithm. The time course of recovery of normalized peak inward currents was best fit with the double exponential function

$$I_2/I_1 = -A_1 \exp(-t/\tau_1) - A_2 \exp(-t/\tau_2) + C \quad (1)$$

where  $I_2$  is the peak inward  $\text{Na}^+$  current of the test pulse during recovery,  $I_1$  is the peak inward  $\text{Na}^+$  current of a test pulse under fully available conditions,  $\tau_1$  and  $\tau_2$  are the time constants of the faster and the slower component of recovery,  $A_1$  and  $A_2$  are the respective amplitudes of these time constants, and  $C$  is the final level of recovery that was 1.0 for all mutants. The time course of development of the ultra-slow inactivated state was best fit with a single exponential function:

$$A_2 = S^\infty(1 - \exp(t/\tau_d)) \quad (2)$$

where  $\tau_d$  is the time constant of development of ultra-slow inactivation and  $S^\infty$  is the final level of ultra-slow inactivation, expressed as a fraction of total inactivation. The quality of fitting recovery from inactivation curves to monoexponential or biexponential functions was evaluated by calculating the  $F$  statistic and significant differences were tested for using the  $F$  distribution with a confidence limit of 95%.

The  $\mu$ -CTX analog R13Q was synthesized by solid state synthesis on a polystyrene-based Rink amide resin on an Applied Biosystems 431A synthesizer. The crude linear peptide was initially desalted on Sephadex G-10/20% acetic acid, then purified by preparative HPLC to ~90% homogeneity as determined by analytical HPLC. After folding of the peptide

by air oxidation,  $\mu$ -CTX R13Q was purified to near-homogeneity by HPLC. The purified peptide was characterized by quantitative amino acid analysis. Owing to the limited precision of weighing lyophilized samples, the absolute concentration is accurate to within  $\pm 10\%$ . As a further check that the folded structure did not deviate from that of the native toxin, 1-dimensional proton NMR spectra were recorded at 15° in aqueous solution containing 5%  $\text{D}_2\text{O}$  at 500 MHz. The proton shifts were similar to those of the native toxin. Qualitative NOE data indicated that the basic secondary structure remained the same. The channel-blocking activity was checked by recording from single  $\text{Na}^+$  channels incorporated in planar bilayers (K. Hui, I. Sierralta, and R. French, unpublished results). For further details, see Chang et al. (1998).

Data are expressed as means  $\pm$  SE. Statistical comparisons were made using the two-tailed Student's  $t$ -tests. A  $p < 0.05$  was considered as being significant.

## RESULTS

The first indication of the presence of a very slow inactivation process was the occurrence of a progressive increase in peak  $\text{Na}^+$  current in *Xenopus* oocytes expressing the mutation K1237E. Typically, oocytes several days after injection of mRNA for these mutants had a resting membrane potential of  $\sim -30$  mV upon initial impalement. After establishing a negative holding potential of  $-120$  mV by voltage clamp, the peak  $\text{Na}^+$  current assessed by consecutive short test pulses increased to a stable level over a several minute period in K1237E, whereas in wild-type  $\mu 1$  a stable current level was reached within  $\sim 60$  s. After the  $\text{Na}^+$  current had stabilized at a higher level, a subsequent prolonged depolarization was followed by a similar slow recovery in K1237E (Fig. 1 A).

### Recovery from ultra-slow inactivation (Fig. 1 B)

$\text{Na}^+$  channels were inactivated by depolarizing clamp steps of 300-s duration to  $-30$  mV from a holding potential of  $-120$  mV. The membrane potential was then returned to the holding potential of  $-120$  mV, and the time course of recovery from inactivation was assessed by applying brief, repetitive (20-ms) test pulses to  $-10$  mV (voltage with peak inward current) at 10- or 20-s intervals in order to measure the extent of recovery. These long test pulse intervals allowed complete recovery of channels from fast inactivation during the interpulse interval. We did not perform a standard double-pulse protocol to assess recovery from pre-pulses of 300-s duration because the time required for such a protocol would have drastically limited data collection.

Peak  $\text{Na}^+$  currents of wild-type  $\mu 1$  and mutant K1237R channels recovered almost completely within  $\sim 60$  s. In contrast to  $\mu 1$  and K1237R, channels carrying the mutations K1237S and K1237E did not completely recover until more than 300 s had elapsed. The calculated time constants of recovery were 9–17 s for  $\tau_1$  and 75–130 s for  $\tau_2$  (Table 1).  $\tau_1$  and  $\tau_2$  most likely represent the time constants of recovery from two distinct inactivated states.  $\tau_2$ , the longer time constant of recovery, corresponded to a component representing  $\sim 20\%$  ( $A_2$  in Table 1) of the overall time course of recovery of  $\mu 1$  and K1237R channels. This component was

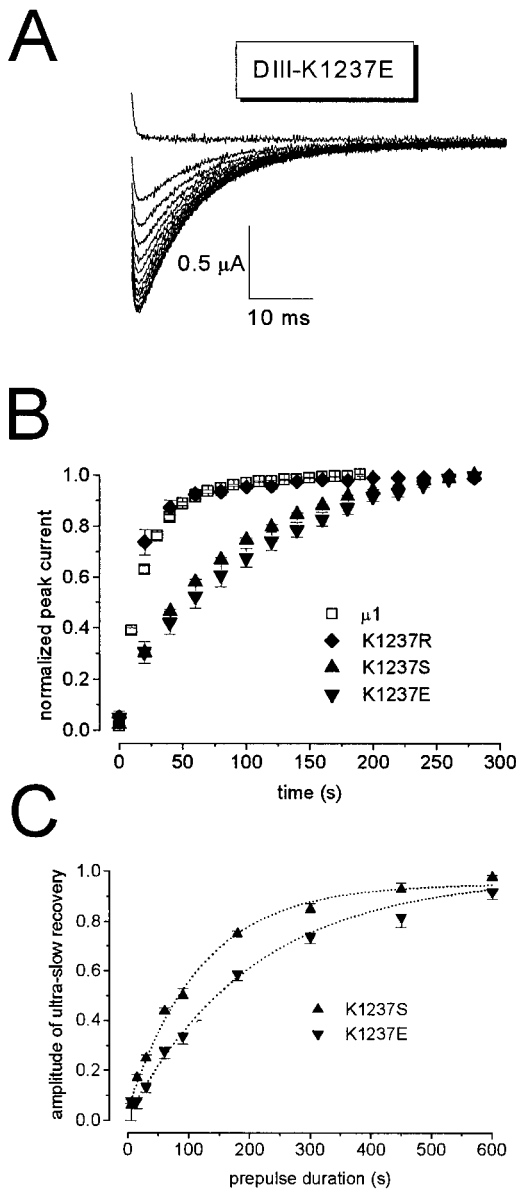


**FIGURE 1** Time course of recovery from ultra-slow inactivation. From a holding potential of  $-120$  mV, the channels were inactivated by a 300-s depolarizing step to  $-30$  mV. After returning to  $-120$  mV, recovery from inactivation was monitored by repetitive test pulses to  $-10$  mV at 20-s intervals with the exception of wild-type  $\mu 1$ , where in order to improve the resolution of the time course of recovery we used 10-s intervals. (A) Slowly increasing inward currents through K1237E channels elicited by test pulses after the holding potential was returned to  $-120$  mV. Test pulse duration was 100 ms, and for better resolution only the first 60 ms of the pulse are shown. (B) Comparison of the time courses of recovery from ultra-slow inactivation in native  $\mu 1$ , and in constructs with mutations at the K1237 site ( $n = 6$  for each data point). Test pulse duration was 20 ms. The mutations in domains III, in which the charge of the residue was altered, exhibited a substantial amount of slow recovery from inactivation, whereas wild-type  $\mu 1$ , and the charge-conserving mutation in domain III, K1237R, recover much faster. (C) The time course of development of ultra-slow inactivation. The membrane potential was depolarized from  $-120$  mV to  $-30$  mV for variable lengths of time, and the time course of recovery at  $-120$  mV was monitored for each prepulse duration as described in the legend to Fig. 1 B. The time course of recovery from ultra-slow inactivation for each prepulse duration was then fitted with two exponentials (Eq. 1). The amplitude of the ultra-slow exponential component of recovery ( $A_2$

**TABLE 1** Parameters of recovery of Na<sup>+</sup> currents after a 300-s prepulse to  $-30$  mV

	$\mu 1$	K1237R	K1237S	K1237E
$\tau_1$	$16.6 \pm 0.6$	$11.2 \pm 2.3$	$10.2 \pm 1.3$	$8.9 \pm 2.9$
$\tau_2$	$76.9 \pm 22.1$	$74.6 \pm 13.7$	$97.5 \pm 7.4$	$129.3 \pm 10.6$
$A_1$	$0.77 \pm 0.07$	$0.79 \pm 0.07$	$0.15 \pm 0.03^*$	$0.2 \pm 0.04^*$
$A_2$	$0.23 \pm 0.07$	$0.21 \pm 0.03$	$0.85 \pm 0.03^*$	$0.8 \pm 0.08^*$

Shown are time constants of recovery from slow inactivation ( $\tau_1$ , s) and ultra-slow inactivation ( $\tau_2$ , s) following a 300-s prepulse to  $-30$  mV, as well as the individual amplitudes ( $A_1, A_2$ ).  $n = 6$  for each construct. For the protocol see legend to Fig. 1.

\* Denotes significant differences from wild-type  $\mu 1$ .

dramatically increased to  $\sim 80\%$  in channels carrying the mutations K1237S and K1237E. This percentage could be increased with longer depolarizing prepulses. More than 90% of the mutant K1237S and K1237E channels could be driven into the ultra-slow inactivated state by increasing the duration of the prepulse in our experiments to 600 s (Fig. 1 C). Because of its long duration,  $\tau_2$  may reflect recovery from a “very slow” inactivation process that was first observed in the squid giant axon (Adelman and Palti, 1969; Rudy, 1978). Fox suggested using the term “ultra-slow” inactivation for inactivated states characterized by time constants in the range of 30–200 s (Fox, 1976). The faster component of recovery ( $A_1$  in Table 1) accounting for  $\sim 80\%$  of recovery of  $\mu 1$  and K1237R channels, and for only 15–20% of recovery of K1237S and K1237E mutants, had a time constant of  $\sim 10$  s ( $\tau_1$  in Table 1). By using standard double-pulse protocols for  $\mu 1$   $\alpha$  subunits expressed in *Xenopus* oocytes, Featherstone et al. (1996) found recovery with a single time constant of  $\sim 10$  s at  $-120$  mV after a 60-s prepulse to 0 mV. Most likely,  $\tau_1$  corresponds to this reported time constant and thus reflects the predominant state of *slow* inactivation that can be induced in wild-type channels. The mutations K1237S and K1237E, however, appear to favor entry into a state of *ultra-slow* inactivation.

### Development of ultra-slow inactivation

The time course of development of the ultra-slow inactivated state during prolonged depolarization is shown in Fig. 1 C. From a holding potential of  $-120$  mV, the membranes were depolarized for variable time periods. After returning to the holding potential, the time course of recovery after each depolarizing step was assessed by repetitive test pulses to  $-10$  mV at 20-s intervals. Then the calculated amplitude

in Eq. 1) is plotted as a function of the respective duration of the inactivating prepulse. The connecting lines are results of single exponential fits to the data points (Eq. 2). The time constants of development of ultra-slow inactivation were  $119.0 \pm 4.9$  s, and  $206.9 \pm 23.3$  s for K1237S and K1237E, respectively. Number of experiments for each duration of the depolarizing prepulse: K1237S: 5 s (2), 15 s (4), 30 s (6), 60 s (7), 90 s (4), 180 s (4), 300 s (7), 450 s (4), 600 s (7). K1237E: 5 s (2), 15 s (7), 30 s (6), 60 s (7), 90 s (3), 180 s (5), 300 s (6), 450 s (4), 600 s (7).

of ultra-slow recovery component ( $A_2$ ), derived from Eq. 1, was plotted as a function of durations of the inactivating prepulses. After a 600-s depolarization, 90–100% of the channels with the mutations K1237S or K1237E had entered an ultra-slow mode. The time constants of development of ultra-slow inactivation at  $-30$  mV were  $119.0 \pm 4.9$  s and  $206.9 \pm 23.3$  s for K1237S and K1237E, respectively.

### Coexpression of the $\beta 1$ subunit

Coexpression of the rat  $\beta 1$  subunit with the  $\alpha$  subunit of the  $\mu 1$  Na<sup>+</sup> channel speeds current decay and accelerates recovery from fast inactivation (Isom et al., 1992; Patton et al., 1994; Nuss et al., 1995; Chang et al., 1996). We tested whether the  $\beta 1$  subunit had an effect on ultra-slow inactivation of the mutant K1237E channel. First, it was necessary to show that the  $\beta 1$  subunit was expressed sufficiently to have its expected effect on fast inactivation by measuring the time course of recovery after a brief (1-s) depolarizing prepulse. The inset to Fig. 2 shows a typical short prepulse experiment with and without  $\beta 1$  subunit coexpression. Channels were depolarized to  $-20$  mV for 1 s and then were allowed to recover for variable test intervals at  $-120$  mV. An interpulse interval of 20 s elapsed between depolarizing pulses to assure complete recovery between pulses. The time course of recovery was fitted with Eq. 1. Care must be taken in comparing the resulting parameters to those derived from analysis of recovery after long (300–600 s) prepulses because the channel is recovering from different inactivation states as a consequence of the different protocol. With short depolarizations  $\tau_1$  and  $\tau_2$  were  $16.7 \pm 5$  ms and  $3924.4 \pm 267.6$  ms if only the  $\alpha$  subunit was expressed ( $n = 6$ ). When the  $\beta 1$  subunit was coexpressed with the  $\alpha$  subunit, both  $\tau_1$  and  $\tau_2$  were reduced:  $4.9 \pm 0.6$  ms and  $1968.0 \pm 892.0$  ms, respectively ( $n = 6$ ;

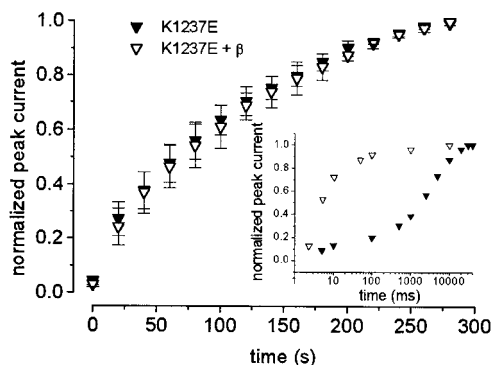


FIGURE 2 The  $\beta 1$  subunit has no effect on ultra-slow inactivation.  $\beta 1$  was coexpressed with the  $\alpha$  subunit carrying the DIII K1237E mutation ( $n = 3$ ). The stimulation protocol is identical to Fig. 1 B. Recovery from ultra-slow inactivation remains unchanged if compared to that seen when the  $\alpha$  subunit is expressed alone ( $n = 3$ ). However, coexpression with  $\beta 1$  accelerated recovery from a 1-s prepulse to  $-20$  mV as assessed with a standard double pulse protocol (inset, data from single oocytes, see text for details).

$p < 0.05$ ). Coexpression of the  $\beta 1$  subunit produced its most dramatic changes in the relative amplitudes of  $\tau_1$  and  $\tau_2$  components, as previously reported (Chang et al., 1996). The amplitude of the slower component ( $A_2$ ) was  $84 \pm 6\%$  if only the  $\alpha$  subunit was expressed. When the  $\beta 1$  subunit was coexpressed with the  $\alpha$  subunit, the slower component was decreased to  $15 \pm 3\%$  ( $p < 0.0001$ ). Thus, coexpression with  $\beta 1$  substantially accelerated recovery after the short (1-s) depolarizing prepulse, confirming the activity of the  $\beta 1$  subunit in these experiments.

Even though the  $\beta 1$  subunit altered recovery from inactivation produced by short depolarizations, recovery from the ultra-slow inactivated state was unchanged by the presence of  $\beta 1$ . Recovery from a long (300-s) prepulse to  $-30$  mV was determined in the mutant K1237E (Fig. 2) in oocytes where expression of the  $\beta 1$  subunit was confirmed by the procedure described above. Ultra-slow inactivation was produced, as shown in Fig. 1 B. Recovery from this ultra-slow inactivation was identical to that of the  $\alpha$  subunit alone, indicating that the molecular mechanism of ultra-slow inactivation was different from the inactivation process that is affected by the  $\beta 1$  subunit.

### Modulation of ultra-slow inactivation by the mutant $\mu$ -conotoxin GIIIA, R13Q

Studies involving site-directed mutagenesis have demonstrated that fast inactivation is mediated by the interaction of a cytoplasmic loop between the third and the fourth domains and some part of the inner vestibule (Stühmer et al., 1989; West et al., 1992; McPhee et al., 1994; Smith and Goldin, 1997). However, the ultra-slow inactivation process seen in our experiments appears to be quite different, and perhaps related to structural rearrangement of the outer vestibule near or involving the K1237 residue. Consequently, a ligand binding within the outer vestibule of the channel pore might interfere with the ultra-slow inactivation process.  $\mu$ -conotoxin GIIIA ( $\mu$ -CTX) is a 22-amino acid peptide toxin that blocks the skeletal muscle Na<sup>+</sup> channel with high affinity (Moczydlowski et al., 1986). Furthermore, a mutant of  $\mu$ -CTX, R13Q, shows residual current of  $\sim 25$ – $30\%$  of the control when the toxin is bound to the channel (French et al., 1996), allowing assessment of channel gating kinetics in the toxin-bound state. The  $K_d$  of  $\mu$ -CTX R13Q binding to the mutant K1237E is  $\sim 10$   $\mu$ M (unpublished data). Fig. 3 shows the effect of a near-saturating ( $\sim 3 \times K_d$ ) concentration of 27  $\mu$ M  $\mu$ -CTX R13Q on the time course of recovery from inactivation by the mutant channel K1237E. During the control period, K1237E channels were depolarized to  $-30$  mV for 300 s and recovery from ultra-slow inactivation was monitored by 20-ms depolarizations from  $-120$  mV to  $-10$  mV at 20-s intervals, as before. Superfusion of 27  $\mu$ M  $\mu$ -CTX R13Q was started, reducing peak inward current by 75–80%. Thereafter, the oocyte was again depolarized to  $-30$  mV for 300 s and recovery of the residual current at  $-120$  mV was assessed as during control. In the

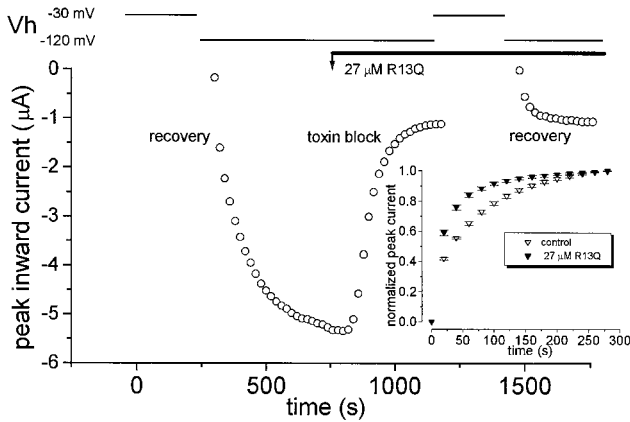


FIGURE 3 Recovery from ultra-slow inactivation in K1237E is modulated by a mutant  $\mu$ -conotoxin known to bind at the outer vestibule. Data points represent peak inward currents elicited by 20-ms step depolarizations to  $-10$  mV from the indicated holding potential (Vh). During a toxin-free control recovery from a 300-s prepulse to  $-30$  mV was monitored analogously to the protocol described for Fig. 1 B. After recovery from ultra-slow inactivation was complete, perfusion with a near-saturating concentration of  $27 \mu\text{M}$   $\mu$ -CTX R13Q was started (arrow, “ $27 \mu\text{M}$  R13Q”). After the reduction of peak Na<sup>+</sup> current by  $\mu$ -CTX R13Q had reached a steady-state level, which reflects the residual current flowing through partially blocked channels, the inactivation/recovery protocol was repeated. Binding of  $\mu$ -CTX R13Q reduced the amount of ultra-slow recovery from inactivation. The inset summarizes the results of six experiments, the peak inward currents were normalized to the level after full recovery. The relative amplitude of ultra-slow component of recovery, as determined by biexponential fits to recovery curves ( $A_2$  in Eq. 1), was  $0.81 \pm 0.05$  under control conditions, and  $0.49 \pm 0.09$  during perfusion with  $27 \mu\text{M}$   $\mu$ -CTX R13Q ( $p < 0.01$ ), while  $\tau_2$  was reduced from  $112.6 \pm 16.8$  s at control to  $66.3 \pm 13.6$  s with  $\mu$ -CTX R13Q ( $p < 0.05$ ).

absence of  $\mu$ -CTX R13Q, recovery was not completed until several hundred seconds following the return to the holding potential. During superfusion with  $\mu$ -CTX R13Q, recovery from ultra-slow inactivation had a much faster time course. The inset to Fig. 3 summarizes six experiments. The data points were normalized to the final level of ultra-slow recovery and the time courses of ultra-slow recovery with and without superfusion with  $\mu$ -CTX R13Q were fitted with Eq. 1. Binding of  $\mu$ -CTX R13Q markedly reduced the amplitude of ultra-slow recovery from inactivation ( $A_2$ ) by  $>30\%$ , from  $0.81 \pm 0.05$  under control conditions to  $0.49 \pm 0.09$  during perfusion with  $27 \mu\text{M}$   $\mu$ -CTX R13Q ( $p < 0.01$ ,  $n = 6$ , Fig. 3).  $\tau_2$  was reduced from  $112.6 \pm 16.8$  s at control to  $66.3 \pm 13.6$  s with  $\mu$ -CTX R13Q ( $p < 0.05$ ). The latter time constant is similar to the time constant of the ultra-slow component of recovery in the wild-type  $\mu 1$  and in the charge preserving mutation K1237R (Table 1).

If  $\mu$ -CTX R13Q directly alters the time course of recovery from ultra-slow inactivation, the toxin should also affect the rate of development of this inactivated state. During superfusion with  $27 \mu\text{M}$   $\mu$ -CTX R13Q the K1237E channels were depolarized from  $-120$  mV to  $-30$  mV for variable lengths of time, and the time course of recovery at  $-120$  mV was monitored for each prepulse duration by applying brief, repetitive (20-ms) test pulses to  $-10$  mV at

20-s intervals. As shown in Fig. 4,  $\mu$ -CTX R13Q significantly slowed the development of ultra-slow inactivation.

If residence of  $\mu$ -CTX R13Q in the channel mouth reduces the probability of the channel being in ultra-slow inactivated state, then the toxin-induced acceleration of recovery from ultra-slow inactivation should be concentration-dependent. This possibility was investigated by gradually reducing the bath concentration of the toxin over a period of 100 min. During wash-out of toxin in K1237E channels, consecutive recovery curves from ultra-slow inactivation were determined. The experiment in Fig. 5 demonstrates that both the toxin-induced reduction in peak inward current and the toxin-induced decrease in the number of channels entering the ultra-slow inactivated state gradually approach control values with similar time courses as the toxin is slowly washed out. This apparent concentration-dependence suggests that the effect of  $\mu$ -CTX R13Q on ultra-slow inactivation is dependent on occupation by R13Q of its blocking site on the channel. The tight inverse correlation between the fraction of channels that are ultra-slow inactivated and the estimated fraction of channels bound by R13Q (Fig. 5 D) supports this contention, but also suggests that, even when a channel is bound, it has a small probability ( $\sim 0.3$ ) of entering the ultra-slow inactivated state. This is close to the probability of ultra-slow inactivation for wild-type channels (see Table 1) in the absence of the peptide.

$\mu$ -CTX R13Q has been shown to shift voltage-dependent channel activation gating, perhaps by an electrostatic effect on the voltage sensor (French et al., 1996). It is, however,

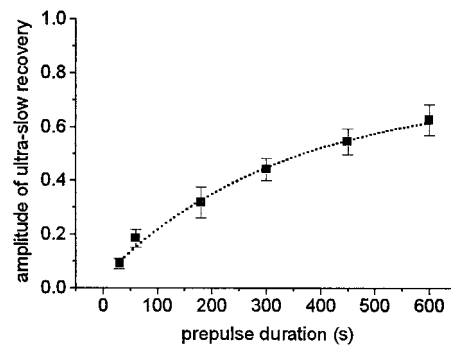
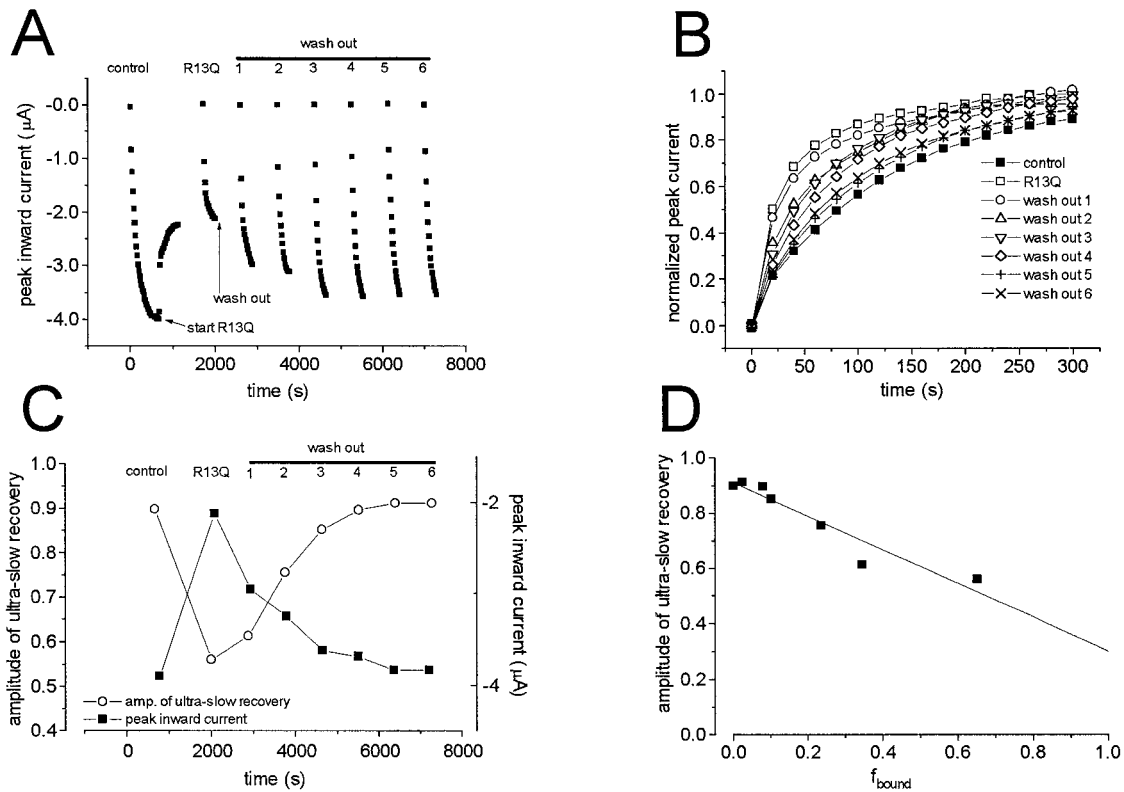


FIGURE 4  $\mu$ -CTX R13Q slows entry into the ultra-slow inactivated state. During superfusion with  $27 \mu\text{M}$   $\mu$ -CTX R13Q, the membrane potential of oocytes expressing K1237E channels was depolarized from  $-120$  mV to  $-30$  mV for variable lengths of time, and the time course of recovery at  $-120$  mV was monitored for each prepulse duration as described in the legend to Fig. 1 B. The time course of recovery from ultra-slow inactivation for each prepulse duration was then fitted with two exponentials (Eq. 1). The amplitude of the ultra-slow exponential component of recovery ( $A_2$  in Eq. 1) is plotted as a function of the respective duration of the inactivating prepulse. The line represents a single exponential fit to the data points (Eq. 2). The time constant of development of ultra-slow inactivation was  $337 \pm 55$  s ( $n = 6$ ). This value was significantly different from the respective value without toxin ( $206 \pm 23$  s;  $p < 0.05$ ; see Fig. 1 C). Hence  $\mu$ -CTX R13Q prolonged entry into the ultra-slow inactivated state consistent with a direct effect of  $\mu$ -CTX R13Q on ultra-slow inactivation.



**FIGURE 5** The effect of  $\mu$ -CTX R13Q on ultra-slow inactivation in the mutant K1237E is dependent on the toxin concentration. (A) Recovery from ultra-slow inactivation was determined during a toxin-free control, during superfusion with  $10 \mu\text{M}$   $\mu$ -CTX R13Q, and, repeatedly, during wash-out of  $\mu$ -CTX R13Q. The data points represent peak inward currents elicited by test pulses during the time course of the experiment. Channels were inactivated by a 600-s prepulse to  $-30$  mV (not shown), then the potential was returned to  $-120$  mV, and recovery from ultra-slow inactivation was monitored at 20-s intervals by repetitive 20-ms test pulses to  $-10$  mV ("control"). After recovery from ultra-slow inactivation was complete, superfusion with  $10 \mu\text{M}$   $\mu$ -CTX R13Q was started (arrow, "start R13Q"). After the toxin-induced reduction of peak inward current had reached a steady-state level, recovery from ultra-slow inactivation was assessed by the same prepulse/test pulse protocol that was used during control. Recovery from ultra-slow inactivation was substantially accelerated by  $\mu$ -CTX R13Q ("R13Q", top). Then, wash-out of the toxin was started (arrow, "wash out"). During wash-out, recovery from ultra-slow inactivation was repeatedly determined by consecutive prepulse-test pulse protocols identical to control. ("wash out" 1–6, top). (B) The normalized values of peak inward current of each time course of recovery from ultra-slow inactivation from the experiment shown in (A) are plotted versus the time after the inactivating prepulse. The time course of recovery from ultra-slow inactivation is substantially accelerated by  $\mu$ -CTX R13Q. This acceleration is gradually reduced during wash-out of the toxin. (C) The values of peak inward current of each time course of recovery from ultra-slow inactivation shown in (A) were fitted with double-exponential functions (Eq. 1). Then, the amplitudes of the ultra-slow components of inactivation recovery were estimated in each case ( $A_2$  in Eq. 1). Panel C shows the amplitudes of the ultra-slow component of recovery from inactivation associated with each recovery curve in (A) [abscissa is identical to (A)]. The amplitude of ultra-slow inactivation correlated with the peak inward current after full recovery, a measure of the toxin remaining. Superfusion with  $\mu$ -CTX R13Q resulted in a decrease of both peak inward current (i.e., toxin block), and in a reduction of the amplitude of ultra-slow recovery from inactivation (i.e., of the number of channels entering the ultra-slow inactivated state). During wash-out toxin block was gradually decreased (return of peak inward current to control values). This effect was mirrored by an increase in the amplitude of recovery from ultra-slow inactivation. Hence, the magnitude of the effect of  $\mu$ -CTX R13Q on ultra-slow inactivation is correlated with a measure of the toxin remaining in the bath. (D) Inverse correlation between the amplitude of ultra-slow inactivation, and the estimated fraction of channels bound by R13Q,  $f_{\text{bound}}$ , from the experiment shown in (A). The occupancy of the channel by  $\mu$ -CTX R13Q was calculated from the current reduction, assuming that 70% of the single channel current is blocked (French et al., 1996:  $f_{\text{bound}} = 1 - [(I/I_{\text{control}}) - 0.3]/0.7$ ). The data can be well-fit with a linear regression ( $R = -0.95$ ;  $p = 0.00019$ ). When  $f_{\text{bound}} = 1$  the regression line predicts an amplitude of ultra-slow recovery of  $\sim 0.3$ , which approximates the amplitude of ultra-slow recovery in wild-type channels (Table 1). Parenthetically, we note that if block of the single channel current for the channel mutant K1237E were all-or-none, rather than only 70% complete, the predicted probability of ultra-slow inactivation for this protocol with all channels R13Q-bound would be decreased slightly to  $\sim 0.15$ . If no peptide is bound, this amplitude is predicted to be between 0.9 and 1.0; which is in agreement with the amplitude of ultra-slow inactivation in K1237E, in the absence of toxin. Overall, the data suggest a close relationship between channel occupancy by the toxin and the removal of ultra-slow inactivation.

worth noting that there was no conclusive evidence for a parallel shift in inactivation (French and Horn, 1997). Nonetheless, the observed reduction of ultra-slow inactivation in the drug-bound state might have resulted from a toxin-induced shift of the inactivation potential and/or the recovery potential. Therefore, we designed a set of experiments to determine whether toxin-induced shifts in gating may ac-

count for the toxin effect on ultra-slow inactivation. Fig. 6 A shows the effect of variations in the potential of a 300 s inactivating prepulse on ultra-slow recovery from inactivation by the mutant channel K1237E. Recovery from ultra-slow inactivation was determined as in the experiments shown in Fig. 1 B, except that the data were acquired during a toxin-free control and during subsequent superfusion with

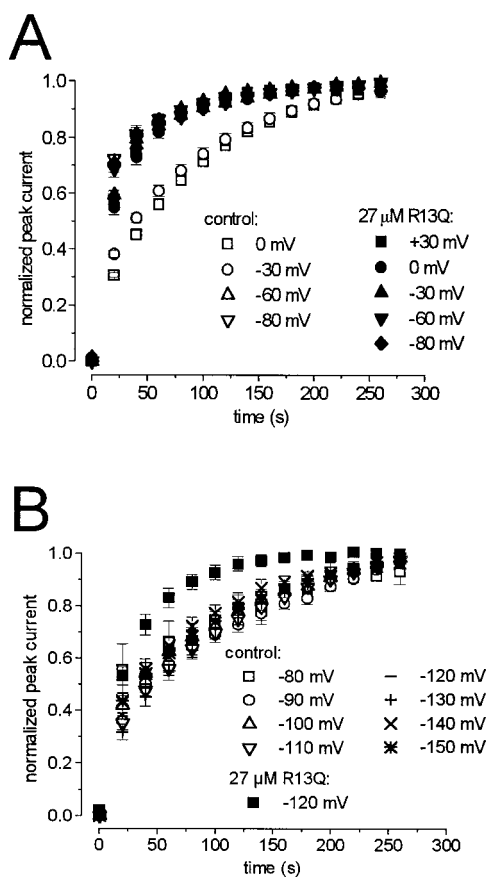


**FIGURE 6** The reduction of ultra-slow inactivation by  $\mu$ -CTX R13Q does not appear to be produced by an electrostatic effect on the voltage sensor. (A) The reduction in the relative amplitude of ultra-slow inactivation by  $\mu$ -CTX R13Q is independent of the prepulse voltage. Recovery at  $-120$  mV from a 300-s prepulse to the indicated potentials was monitored in K1237E during a drug-free control, and during perfusion with  $27 \mu\text{M}$   $\mu$ -CTX R13Q. The reduction of ultra-slow recovery from inactivation by  $\mu$ -CTX R13Q was similar for prepulse potentials of  $+30$  mV,  $0$  mV, and  $-30$  mV. Little change with  $\mu$ -CTX R13Q was observed at more negative potentials ( $-60$  mV,  $-80$  mV) where only small amounts of ultra-slow recovery were observed under control conditions (overlap of symbols for control with data points acquired during superfusion with  $\mu$ -CTX R13Q). No controls were obtained for the prepulse potential  $+30$  mV because of the difficulty to maintain stable clamp conditions for prolonged periods at very depolarized potentials. Number of experiments (control/ $\mu$ -CTX R13Q):  $+30$  mV (0/5),  $0$  mV (8/8),  $-30$  mV (11/11),  $-60$  mV (6/6), and  $-80$  mV (6/6). (B) The reduction of ultra-slow inactivation by  $\mu$ -CTX R13Q in K1237E cannot be reproduced by changes in recovery potential. Recovery from a 300-s prepulse to  $-30$  mV was monitored analogously to the protocol in Fig. 1 B at different recovery potentials (mV/number of experiments):  $-90/8$ ,  $-100/9$ ,  $-110/8$ ,  $-120/13$ ,  $-130/8$ ,  $-140/5$ ,  $-150/3$ . The time courses of the recovery from ultra-slow inactivation show little dependence on the investigated recovery potentials. The  $\mu$ -CTX R13Q-induced reduction of ultra-slow inactivation at a recovery potential of  $-120$  mV (R13Q,  $27 \mu\text{M}$ ; same data as inset to Fig. 3, after  $\mu$ -CTX R13Q) could not be reproduced by changing the recovery potential under drug-free conditions. Thus, toxin-induced shifts in recovery potential are unlikely to account for the reduction in ultra-slow inactivation by  $\mu$ -CTX R13Q.

$27 \mu\text{M}$   $\mu$ -CTX R13Q. Presence of the toxin substantially reduced the amplitude of the ultra-slow recovery component from inactivation after prepulses to  $+30$  mV,  $0$  mV, and

$-30$  mV. Thus, a toxin-induced shift of the inactivation potential cannot account for the reduction in ultra-slow inactivation by  $\mu$ -CTX R13Q.

Fig. 6 B shows the effect of variations in the recovery potential on ultra-slow recovery from inactivation. A 300-s prepulse to  $-30$  mV was introduced after which the potential was returned to values between  $-90$  mV and  $-150$  mV. Recovery from ultra-slow inactivation at the indicated potentials was assessed as described for Fig. 1 B. Time course and amplitude of recovery from ultra-slow inactivation had no substantial voltage-dependence between  $-90$  mV and  $-150$  mV. Even at these very negative recovery potentials a substantial number of channels recovered in an ultra-slow fashion. By comparison, superfusion with  $\mu$ -CTX R13Q reduced the number of channels recovering in an ultra-slow fashion at  $-120$  mV much more than any change in recovery potential. Therefore, it is unlikely that an electrostatic influence of the toxin on the voltage sensor during recovery accounts for the toxin-induced reduction in ultra-slow recovery. These results support the hypothesis that  $\mu$ -CTX R13Q interferes with ultra-slow inactivation by means of a direct interaction with the outer vestibule.

An additional inference may be drawn from the data in Fig. 6. The results argue against a strong voltage-dependence of  $\mu$ -CTX R13Q binding under our experimental conditions. If binding were significantly voltage-dependent, that would necessarily result in a voltage-dependence of its inhibition of ultra-slow recovery. Block of open, batrachotoxin-modified Na<sup>+</sup> channels by various  $\mu$ -CTX derivatives is clearly voltage-dependent (Becker et al., 1992), as is block by the guanidinium toxins, tetrodotoxin (TTX) and saxitoxin (STX) (Moczydlowski et al., 1984a, b). However, the voltage-dependence of TTX and STX block measured by allowing the block to equilibrate with closed channels at negative holding potentials is significantly less (Satin et al., 1994). Thus, the lack of voltage-dependence of the  $\mu$ -CTX R13Q effect in our experiments appears to reflect the lower voltage sensitivity of the interaction of these blocking toxins with closed Na<sup>+</sup> channels in the absence of batrachotoxin.

**DISCUSSION**

We have shown that there is a very slow component of the inactivation of  $\mu\text{I}$  Na<sup>+</sup> channels. If channels are depolarized to  $-30$  mV for 300 s,  $\sim 20\%$  of the wild-type channels enter into this “very slow” inactivation process. However, replacement of K1237, a channel residue involved in the selectivity process, by either serine or glutamic acid dramatically increased the very slow component to  $\sim 80\%$  of the overall inactivation process under our standard protocols. Time constants of entry into and exit from this state were 100–200 s. A very slow inactivation process has been described for squid giant axon Na<sup>+</sup> channels (Adelman and Palti, 1969; Rudy, 1978), called “ultra-slow” inactivation by Fox (1976), and probably underlies the requirement for prolonged, strong hyperpolarization to observe voltage ac-

tivation of channels purified and reconstituted from eel electric organ (Correa et al., 1990). The similarity of the time constants of that process with the one we observed with the  $\mu 1$  K1237S and K1237E mutations led us to use Fox's terminology. In contrast to the mutations K1237S and K1237E, the charge-preserving mutation K1237R did not increase the component of the ultra-slow inactivation process. Thus, alteration of charge at the K1237 position favored entry of the channels into ultra-slow inactivation by long depolarizations.

There are several lines of evidence that ultra-slow inactivation is a unique state. In our standard protocol, depolarizations shorter than 600 s yielded a biexponential recovery time course, with an additional faster time constant of  $\sim 10$  s. The inactivated state with this more rapid recovery and with this smaller time constant may correspond to "slow" inactivation, which has been repeatedly observed in wild-type  $\text{Na}^+$  channels (Nuss et al., 1995, 1996; Featherstone et al., 1996). Slow inactivation can be produced in  $\mu 1$   $\text{Na}^+$  channel  $\alpha$  subunits by depolarizing prepulses as short as 1-s duration. If the time course of recovery of peak  $\text{Na}^+$  inward current following such short prepulses is fitted with two exponentials, the calculated time constants are on the order of several milliseconds ("fast inactivation") and on the order of several seconds ("slow inactivation"; Balser et al., 1996). In the mutant K1237E, recovery from inactivation produced by a short (1-s) depolarizing prepulse also follows a double-exponential time course, suggesting states analogous to both fast and slow inactivation in this mutant (Fig. 2). Hence, the mutation does not appear to produce any substantial abnormalities in recovery from short depolarizations.

### Coexpression with the $\beta 1$ subunit

A second line of evidence is that coexpression of the  $\beta 1$  subunit with the  $\alpha$  subunit affects slow inactivation, but not ultra-slow inactivation. Wild-type  $\mu 1$   $\text{Na}^+$  channels show a substantial amount of slow inactivation when the  $\alpha$  subunit is expressed alone in *Xenopus* oocytes. Coexpression of the  $\beta 1$  subunit reduces the number of channels entering a slow inactivation process and speeds their recovery (Zhou et al., 1991; Balser et al., 1996; Chang et al., 1996). The mechanism of this  $\beta 1$  subunit effect is not completely understood. The  $\beta 1$  subunit may affect folding of the  $\alpha$  subunit during cytoplasmic processing, or it may interact with the inactivation process after membrane insertion of the channel. As shown in Fig. 2, the amount of slow inactivation (but not ultra-slow inactivation) in the mutant K1237E is also substantially reduced by coexpression with the  $\beta 1$  subunit. This again indicates that the mutation itself does not corrupt the mechanism of the fast and slow components of inactivation. In contrast, the  $\beta 1$  subunit fails to influence the ultra-slow inactivation process seen with the K1237 mutants, implying that the mechanism of ultra-slow inactivation is different from that of fast inactivation.

### Comparison to C-type inactivation of $\text{K}^+$ channels

$\text{K}^+$  channels have several inactivation mechanisms (Choi et al., 1991). Fast inactivation is associated with the cytoplasmic N-terminus, and can be removed by deletion of critical parts of that segment, thereby revealing a second, slower inactivation process that has been called C-type inactivation (Hoshi et al., 1991). This slow inactivation process is modified by external tetraethylammonium ( $\text{TEA}^+$ ) block (Grissmer and Cahalan, 1989; Choi et al., 1991) and external  $\text{K}^+$  (López-Barneo et al., 1993; Baukowitz and Yellen, 1995). Mutations of residues in the external mouth of the  $\text{K}^+$  channel alter this C-type inactivation (Hoshi et al., 1991; López-Barneo et al., 1993).

C-type inactivation appears to involve structural rearrangements of the  $\text{K}^+$  channel outer vestibule. When T449 of *Shaker* is mutated to cysteine, C-type inactivation is modulated by state-dependent binding/block by  $\text{Cd}^{2+}$  or  $\text{Zn}^{2+}$  (Yellen et al., 1994). Cysteine at position 449 and cysteine substitutions at positions 448 or 450 are dramatically more reactive with sulfhydryl reagents when the channel is in the C-type inactivation state, and C448 can spontaneously form disulfide bonds in the inactivated state (Liu et al., 1996). These and other observations have been interpreted to indicate that C-type inactivation requires a structural rearrangement of the outer pore of the channel, and that blocking ions or molecules can modify the inactivation process by binding in the critical region.

In  $\text{Na}^+$  channels, fast inactivation is also mediated by an intracellular structure: the domains III-IV linker (West et al., 1992). However, it is plausible to consider that the ultra-slow inactivation process revealed by the K1237 mutations might be related to a structural rearrangement on the  $\text{Na}^+$  channel outer mouth in an analogous way to that of  $\text{K}^+$  channel C-type inactivation. We tested this idea by examining the effect of block with a  $\text{Na}^+$  channel blocking ligand on ultra-slow inactivation.

### Block of ultra-slow inactivation by $\mu$ -CTX R13Q

Several molecules are known to block the  $\text{Na}^+$  channel by binding in the outer channel vestibule. The guanidinium toxins tetrodotoxin (TTX) and saxitoxin (STX) interact with multiple residues in the outer mouth (Terlau et al., 1991). However, their affinities are markedly reduced by K1237 mutations and they completely block the currents.  $\mu$ -CTX GIIIA blocks skeletal muscle  $\text{Na}^+$  channels with high affinity, and its binding site is also in the channel's outer vestibule (Cruz et al., 1985; Moczydlowski et al., 1986; Becker et al., 1992; Dudley et al., 1995; French et al., 1996; Chang et al., 1998). The toxin mutant  $\mu$ -CTX R13Q has the interesting property that binding only partially occludes the channel, reducing but not abolishing single channel current (Becker et al., 1992; French et al., 1996; Chang et al., 1998). Therefore, the effect of its binding on channel gating kinetics can be monitored by recording this residual current. In

Na<sup>+</sup> channels with the K1237E mutation we found that this molecule destabilized the ultra-slow inactivated state both by slowing entry into the state (Fig. 4) and accelerating exit from the state (Fig. 3). The concentration-dependence of the toxin effect on ultra-slow recovery (Fig. 5) suggested that  $\mu$ -CTX R13Q was affecting only toxin bound channels. Also, this effect was independent of a range of prepulse and recovery potentials too large to be explained by an electrostatic influence of the charged toxin on the nearby voltage-sensing systems or the surface potential (Fig. 6; French et al., 1996). The data are consistent with the idea that binding of  $\mu$ -CTX R13Q to the channel mutant K1237E favors a conformation of the channel which, with respect to ultra-slow inactivation, behaves very much like the wild-type channel in the absence of the peptide.

The reduction of ultra-slow inactivation by  $\mu$ -CTX R13Q in K1237E may be analogous to the effects of TEA<sup>+</sup> and K<sup>+</sup> on C-type inactivation in *Shaker* K<sup>+</sup> channels. The mechanism of  $\mu$ -CTX R13Q is unclear, however. One possibility is that  $\mu$ -CTX may physically impede structural changes in the Na<sup>+</sup> channel vestibule involved in generating the ultra-slow inactivated state. If  $\mu$ -CTX R13Q affects a structural rearrangement, it is unlikely that the effect is directly on K1237. Mutant cycle analysis shows that the strongest interactions of  $\mu$ -CTX R13 with the outer vestibule are extracellular to K1237 and with E403 and E758 (Dudley et al., 1995; Chang et al., 1998). Consequently, structural rearrangements prevented by  $\mu$ -CTX R13Q are more likely to be produced by widespread interactions of the toxin with the outer vestibule of the channel.

### Mechanism of ultra-slow inactivation

K1237 has been identified as part of the selectivity apparatus of the channel. Terlau et al. (1991) initially proposed that one residue from each of the four P loops—D400, E755, K1237, and A1529—are adjacent in the pore and play a critical role in ion permeation. Their evidence was that these residues are important for TTX and STX binding and block, for channel conductance, and for selectivity (Heinemann et al., 1992). This proposal has received considerable support from additional mutational studies of the Na<sup>+</sup> channel (Chiamvimonvat et al., 1996a; Chang et al., 1998; Tsushima et al., 1997), from modeling of the molecular structure of the outer vestibule (Lipkind and Fozzard, 1994), and from mutation of analogous residues in the Ca<sup>2+</sup> channel P loops (Yang et al., 1993; Ellinor et al., 1995; Schlieff et al., 1996). K1237 was shown to be the key residue regulating ion selectivity in the Na<sup>+</sup> channel (Favre et al., 1996) and permeation (Sun et al., 1997). These residues also control access of outside local anesthetic drugs to their inner pore binding site (Sunami et al., 1997).

Sun et al. (1997) have hypothesized that K1237 interacts with the adjacent carboxyl residues in the selectivity ring to determine the physical size of the narrow opening and to create the electrostatic and chemical milieu necessary for

ion recognition and permeation. Our results underline the importance of K1237 in channel function. We find that changing the charge at this position permits development of a non-conducting state of the channel from which recovery even at hyperpolarized potentials is very slow. One mechanism by which the charge in position 1237 might stabilize the structure of the outer vestibule is through salt-bridge formation or through other interactions with nearby residues, and study of combinations of mutations may provide further insight into a molecular mechanism. It is not difficult to imagine that a conformational change in this critical part of the pore could render the channel non-conducting.

The loss of channel selectivity is not completely linked to ultra-slow inactivation, however. Recently, it has been demonstrated that replacement of extracellular Na<sup>+</sup> ions by impermeant ions reduces the open probability of Na<sup>+</sup> channels (Townsend et al., 1997) and enhances their slow inactivation (Townsend and Horn, 1997). These data strongly suggest that permeant ions can themselves influence the channel structure (Yellen, 1997). We ask whether ultra-slow inactivation, favored by mutations of K1237, is linked to the change in the permeation properties of the channel that are also produced by this mutation. Favre et al. (1996) found that the charge-preserving mutation K1237R caused loss of selectivity between Na<sup>+</sup> and K<sup>+</sup>. However, our study demonstrated that this mutation did not produce ultra-slow inactivation. Based upon the known interactions of the toxin with the channel, the modifying effect of  $\mu$ -CTX R13Q is not likely to be by a direct interaction with the residue at position 1237, but rather at a more superficial site. This suggests that the conformational stability conferred by K1237 may broadly involve the vestibule. In this regard the modification of ultra-slow inactivation by  $\mu$ -CTX R13Q in Na<sup>+</sup> channels may be different from the effect of TEA<sup>+</sup> on C-type inactivation in *Shaker* K<sup>+</sup> channels. TEA<sup>+</sup> appears to inhibit C-type inactivation only if it enters deeply into the pore (Molina et al., 1997). C-type inactivation has thus been suggested to involve a conformational change restricted to a local site in the pore (Molina et al., 1997) and TEA<sup>+</sup> may act as a “foot in the door” to impede a localized pore closure. Ultra-slow inactivation in Na<sup>+</sup> channels, however, appears to be caused by a more complex rearrangement of the outer pore of the channel.  $\mu$ -CTX R13Q may act as a “splint” in the outer vestibule, stabilizing the structure of this region of the channel.

The authors thank Yu Huang, Bei Li, and Gayle Tonkovich for their technical assistance, and Dr. Jonathan Satin for helpful discussions. Thanks are due to Dr. Denis McMaster of the Peptide Synthesis Laboratory, University of Calgary Faculty of Medicine, for providing the peptide  $\mu$ -CTX R13Q.

This work was supported by HL-P01-20592 from the National Institutes of Health and by a grant from the Max Kade Foundation, Inc., New York (to H.T.). Research support was also provided by the Medical Research Council of Canada (MRC), and R.J.F. received salary support as an MRC Distinguished Scientist and a Medical Scientist of the Alberta Heritage Foundation for Medical Research.

## REFERENCES

- Adelman, W. J., and Y. Palti. 1969. The effects of external potassium and long duration voltage conditioning on the amplitude of sodium currents in the giant axon of the squid, *Loglio pealei*. *J. Gen. Physiol.* 54: 589–606.
- Balsler, J. R., H. B. Nuss, N. Chiamvimonvat, M. T. Pérez-García, E. Marban, and G. F. Tomaselli. 1996. External pore residue mediates slow inactivation in  $\mu$ 1 rat skeletal muscle sodium channels. *J. Physiol. (Lond.)* 494:431–442.
- Baukowitz, T., and G. Yellen. 1995. Modulation of  $K^+$  current by frequency and external  $[K^+]$ : a tale of two inactivation mechanisms. *Neuron*. 15:951–960.
- Becker, S., E. Prusak-Sochaczewski, G. Zamponi, A. G. Beck-Sickinger, R. D. Gordon, and R. J. French. 1992. Action of derivatives of  $\mu$ -conotoxin GIIIA on sodium channels. Single amino acid substitutions in the toxin separately affect association and dissociation rates. *Biochemistry*. 31:8229–8238.
- Bowman, S., J. A. Tischfield, and P. J. Stambrook. 1990. An efficient and simplified method for producing site-directed mutations by PCR. *Technique*. 2:254–260.
- Chang, N. S., R. J. French, G. Lipkind, H. A. Fozzard, and S. C. Dudley, Jr. 1998. Predominant interactions between  $\mu$ -conotoxin Arg-13 and the skeletal muscle  $Na^+$  channel localized by mutant cycle analysis. *Biochemistry*. 37:4407–4419.
- Chang, S. Y., J. Satin, and H. A. Fozzard. 1996. Modal behavior of the  $\mu$ 1  $Na^+$  channel and effects of coexpression of the  $\beta$ 1 subunit. *Biophys. J.* 70:2581–2592.
- Chiamvimonvat, N., M. T. Pérez-García, R. Ranjan, E. Marban, and G. F. Tomaselli. 1996b. Depth asymmetries of the pore-lining segments of the  $Na^+$  channel revealed by cysteine mutagenesis. *Neuron*. 16:1037–1047.
- Chiamvimonvat, N., M. T. Pérez-García, G. F. Tomaselli, and E. Marban. 1996a. Control of ion flux and selectivity by negatively charged residues in the outer mouth of rat sodium channels. *J. Physiol. (Lond.)* 491: 51–59.
- Choi, K. L., R. W. Aldrich, and G. Yellen. 1991. Tetraethylammonium blockade distinguishes two inactivation mechanisms in voltage-activated  $K^+$  channels. *Proc. Natl. Acad. Sci. USA*. 88:5092–5095.
- Correa, A. M., F. Bezanilla, and W. S. Agnew. 1990. Voltage activation of purified eel sodium channels reconstituted into artificial liposomes. *Biochemistry*. 29:6230–6240.
- Cruz, L. J., W. R. Gray, B. M. Olivera, R. D. Zeikus, L. Kerr, D. Yoshikami, and E. Moczydlowski. 1985. *Conus geographus* toxins that discriminate between neuronal and muscle sodium channels. *J. Biol. Chem.* 260:9280–9288.
- Dudley, S. C., Jr., H. Todt, G. Lipkind, and H. A. Fozzard. 1995. A  $\mu$ -conotoxin-insensitive  $Na^+$  channel mutant: possible localization of a binding site at the outer vestibule. *Biophys. J.* 69:1657–1665.
- Ellinor, P. T., J. Yang, W. A. Sather, J. F. Zhang, and R. W. Tsien. 1995.  $Ca^{2+}$  channel selectivity at a single locus for high-affinity  $Ca^{2+}$  interactions. *Neuron*. 15:1121–1132.
- Favre, I., E. Moczydlowski, and L. Schild. 1996. On the structural basis for ionic selectivity among  $Na^+$ ,  $K^+$ , and  $Ca^{2+}$  in the voltage-gated sodium channel. *Biophys. J.* 71:3110–3125.
- Featherstone, D. E., J. E. Richmond, and P. C. Ruben. 1996. Interaction between fast and slow inactivation in Skm1 sodium channels. *Biophys. J.* 71:3098–3109.
- Fox, J. M. 1976. Ultra-slow inactivation of the ionic currents through the membrane of myelinated nerve. *Biochim. Biophys. Acta*. 426:232–244.
- French, R. J., and R. Horn. 1997. Shifts of macroscopic current activation in partially blocked sodium channels. Interaction between the voltage sensor and a  $\mu$ -conotoxin. In *From Ion Channels to Cell-to-Cell Conversations*. R. Latorre and J. Saez, editors. Plenum Press, New York. 67–89.
- French, R. J., E. Prusak-Sochaczewski, G. W. Zamponi, S. Becker, A. S. Kularatna, and R. Horn. 1996. Interactions between a pore-blocking peptide and the voltage sensor of the sodium channel: an electrostatic approach to channel geometry. *Neuron*. 16:407–413.
- Grissmer, S., and M. Cahalan. 1989. TEA prevents inactivation while blocking open  $K^+$  channels in human T lymphocytes. *Biophys. J.* 55:203–206.
- Guy, H. R., and F. Conti. 1990. Pursuing the structure and function of voltage-gated channels. *Trends Neurol. Sci.* 13:201–206.
- Heinemann, S. H., H. Terlau, W. Stühmer, K. Imoto, and S. Numa. 1992. Calcium channel characteristics conferred on the sodium channel by single mutations. *Nature*. 356:441–443.
- Hoshi, T., W. N. Zagotta, and R. W. Aldrich. 1991. Two types of inactivation in *Shaker*  $K^+$  channels: effects of alterations in the carboxy-terminal region. *Neuron*. 7:547–556.
- Isom, L. L., K. S. De Jongh, D. E. Patton, B. F. Reber, J. Offord, H. Charbonneau, K. Walsh, A. L. Goldin, and W. A. Catterall. 1992. Primary structure and functional expression of the  $\beta$ 1 subunit of the rat brain sodium channel. *Science*. 256:839–842.
- Lipkind, G. M., and H. A. Fozzard. 1994. A structural model of the tetrodotoxin and saxitoxin binding site of the  $Na^+$  channel. *Biophys. J.* 66:1–13.
- Liu, Y., M. E. Jurman, and G. Yellen. 1996. Dynamic rearrangement of the outer mouth of a  $K^+$  channel during gating. *Neuron*. 16:859–867.
- López-Barneo, J., T. Hoshi, S. H. Heinemann, and R. W. Aldrich. 1993. Effects of external cations and mutations in the pore region on C-type inactivation of *Shaker* potassium channels. *Receptors and Channels*. 1:61–71.
- Makielski, J. C., J. T. Limberis, S. Y. Chang, Z. Fan, and J. W. Kyle. 1996. Coexpression of  $\beta$ 1 with cardiac sodium channel  $\alpha$  subunits in oocytes decreases lidocaine block. *Mol. Pharmacol.* 49:30–39.
- McPhee, J. C., D. S. Ragsdale, T. Scheuer, and W. A. Catterall. 1994. A mutation in segment IVS6 disrupts fast inactivation of sodium channels. *Proc. Natl. Acad. Sci. USA*. 91:12346–12350.
- Moczydlowski, E., S. S. Garber, and C. Miller. 1984a. Batrachotoxin-activated sodium channels in planar lipid bilayers: competition of tetrodotoxin block by  $Na^+$ . *J. Gen. Physiol.* 84:665–686.
- Moczydlowski, E., S. Hall, S. S. Garber, G. R. Strichartz, and C. Miller. 1984b. Voltage dependent blockade of muscle  $Na^+$  channels by guanidinium toxins: Effect of toxin charge. *J. Gen. Physiol.* 84:687–704.
- Moczydlowski, E., B. M. Olivera, W. R. Gray, and G. R. Strichartz. 1986. Discrimination of muscle and neuronal Na-channel subtypes by binding competition between [ $^3H$ ]saxitoxin and  $\mu$ -conotoxins. *Proc. Natl. Acad. Sci. USA*. 83:5321–5325.
- Molina, A., A. G. Castellano, and J. López-Barneo. 1997. Pore mutations in *Shaker*  $K^+$  channels distinguish between the sites of tetraethylammonium blockade and C-type inactivation. *J. Physiol. (Lond.)* 499: 361–367.
- Nuss, H. B., J. R. Balsler, D. W. Orias, J. H. Lawrence, G. F. Tomaselli, and E. Marban. 1996. Coupling between fast and slow inactivation revealed by analysis of a point mutation (F1304Q) in  $\mu$ 1 rat skeletal muscle sodium channels. *J. Physiol. (Lond.)* 494:411–429.
- Nuss, H. B., N. Chiamvimonvat, M. T. Pérez-García, G. F. Tomaselli, and E. Marban. 1995. Functional association of the  $\beta$ 1 subunit with human cardiac (hH1) and rat skeletal muscle ( $\mu$ 1) sodium channel  $\alpha$  subunits expressed in *Xenopus* oocytes. *J. Gen. Physiol.* 106:1171–1191.
- Patton, D. E., L. L. Isom, W. A. Catterall, and A. L. Goldin. 1994. The adult rat brain  $\beta$ 1 subunit modifies activation and inactivation gating of multiple sodium channel  $\alpha$  subunits. *J. Biol. Chem.* 269:17649–17655.
- Pérez-García, M. T., N. Chiamvimonvat, E. Marban, and G. F. Tomaselli. 1996. Structure of the sodium channel pore revealed by serial cysteine mutagenesis. *Proc. Natl. Acad. Sci. USA*. 93:300–304.
- Rudy, B. 1978. Slow inactivation of the sodium conductance in squid giant axons. Pronase resistance. *J. Physiol. (Lond.)* 283:1–21.
- Satin, J., J. T. Limberis, J. W. Kyle, R. B. Rogart, and H. A. Fozzard. 1994. The saxitoxin/tetrodotoxin binding site on cloned rat brain IIa Na channels is in the transmembrane electric field. *Biophys. J.* 67:1007–1014.
- Schlieff, T., R. Schoenherr, K. Imoto, and S. H. Heinemann. 1996. Pore properties of rat brain II sodium channels mutated in the selectivity filter domain. *Eur. Biophys. J.* 25:75–91.
- Smith, M. R., and A. L. Goldin. 1997. Interaction between the sodium channel inactivation linker and domain III S4–S5. *Biophys. J.* 73: 1885–1895.
- Stühmer, W., F. Conti, H. Suzuki, X. D. Wang, M. Noda, N. Yahagi, H. Kubo, and S. Numa. 1989. Structural parts involved in activation and inactivation of the sodium channel. *Nature*. 339:597–603.

- Sun, Y., I. Favre, L. Schild, and E. Moczydlowski. 1997. On the structural basis for size-selective permeation of organic cations through the voltage-gated sodium channel: effect of alanine mutations at the DEKA locus on selectivity, inhibition by Ca<sup>2+</sup> and H<sup>+</sup>, and molecular sieving. *J. Gen. Physiol.* 110:693–715.
- Sunami, A., S. C. Dudley, Jr., and H. A. Fozzard. 1997. Sodium channel selectivity filter regulates antiarrhythmic drug binding. *Proc. Natl. Acad. Sci. USA.* 94:14126–14131.
- Terlau, H., S. H. Heinemann, W. Stühmer, M. Pusch, F. Conti, K. Imoto, and S. Numa. 1991. Mapping the site of block by tetrodotoxin and saxitoxin of sodium channel II. *FEBS. Lett.* 293:93–96.
- Todt, H., S. Dudley, and H. Fozzard. 1997a. Ultra-slow inactivation in the skeletal muscle sodium channel is influenced by pore residues. *Biophys. J.* 72:261a.(Abstr).
- Todt, H., S. C. Dudley, R. J. French, and H. A. Fozzard. 1997b. Evidence in a Na<sup>+</sup> channel for a process analogous to K<sup>+</sup> channel C-type inactivation. *Pflugers Arch.* 434:R110.
- Tomaselli, G. F., N. Chiamvimonvat, H. B. Nuss, J. R. Balsler, M. T. Pérez-García, R. H. Xu, D. W. Orias, P. H. Backx, and E. Marban. 1995. A mutation in the pore of the sodium channel alters gating. *Biophys. J.* 68:1814–1827.
- Townsend, C., H. A. Hartmann, and R. Horn. 1997. Anomalous effect of permeant ion concentration on peak open probability of cardiac Na<sup>+</sup> channels. *J. Gen. Physiol.* 110:11–21.
- Townsend, C., and R. Horn. 1997. Effect of alkali metal cations on slow inactivation of cardiac Na<sup>+</sup> channels. *J. Gen. Physiol.* 110:23–33.
- Trimmer, J. S., S. S. Cooperman, S. A. Tomiko, J. Y. Zhou, S. M. Crean, M. B. Boyle, R. G. Kallen, Z. H. Sheng, R. L. Barchi, F. J. Sigworth, R. H. Goodman, W. S. Agnew, and G. Mandel. 1989. Primary structure and functional expression of a mammalian skeletal muscle sodium channel. *Neuron.* 3:33–49.
- Tsushima, R. G., R. A. Li, and P. H. Backx. 1997. Altered ionic selectivity of the sodium channel revealed by cysteine mutations within the pore. *J. Gen. Physiol.* 109:463–475.
- West, J. W., D. E. Patton, T. Scheuer, Y. Wang, A. L. Goldin, and W. A. Catterall. 1992. A cluster of hydrophobic amino acid residues required for fast Na<sup>+</sup>-channel inactivation. *Proc. Natl. Acad. Sci. USA.* 89:10910–10914.
- Yang, J., P. T. Ellinor, W. A. Sather, J. F. Zhang, and R. W. Tsien. 1993. Molecular determinants of Ca<sup>2+</sup> selectivity and ion permeation in L-type Ca<sup>2+</sup> channels. *Nature.* 366:158–161.
- Yellen, G. 1997. Single channel seeks permeant ion for brief but intimate relationship. *J. Gen. Physiol.* 110:83–85.
- Yellen, G., D. Sodickson, T. Y. Chen, and M. E. Jurman. 1994. An engineered cysteine in the external mouth of a K<sup>+</sup> channel allows inactivation to be modulated by metal binding. *Biophys. J.* 66:1068–1075.
- Zhou, J. Y., J. F. Potts, J. S. Trimmer, W. S. Agnew, and F. J. Sigworth. 1991. Multiple gating modes and the effect of modulating factors on the  $\mu$ I sodium channel. *Neuron.* 7:775–785.